Microchemical Journal 138 (2018) 472–487

Contents lists available at ScienceDirect

Microchemical Journal

journal homepage: www.elsevier.com/locate/microc

Ancient encaustic: An experimental exploration of technology, ageing behaviour and approaches to analytical investigation

R.J. Stacey [a,*], J. Dyer [a], C. Mussell [a], A. Lluveras-Tenorio [b], M.P. Colombini [b,c], Celia Duce [b], Jacopo La Nasa [b], Emma Cantisani [c], S. Prati [d], G. Sciutto [d], R. Mazzeo [d], S. Sotiropoulou [e], F. Rosi [f], C. Miliani [f], L. Cartechini [f], J. Mazurek [g], M. Schilling [g]

[a] Department of Scientific Research, The British Museum, Great Russell St, London, WC1B 3DG, UK
[b] Dipartimento di Chimica e Chimica Industriale, Università di Pisa, Via Giuseppe Moruzzi, 13, 56124 Pisa, Italy
[c] ICVBC-CNR, Via Madonna del Piano 10 - Edificio C, Sesto Fiorentino, 50019 Florence, Italy
[d] Microchemistry and Microscopy Art Diagnostic Laboratory (M2ADL), University of Bologna - Ravenna Campus, via Guaccimanni 42, 48100 Ravenna, Italy
[e] Ormylia Foundation, Art Diagnosis Centre, Ormylia 63071, Greece
[f] CNR-ISTM, Via Elce di Sotto, 8, 06123 Perugia, Italy
[g] The Getty Conservation Institute, 1200 Getty Center Drive, Suite 700, Los Angeles, CA 90049-1684, USA

ARTICLE INFO

Article history:
Received 30 August 2017
Received in revised form 18 December 2017
Accepted 24 January 2018
Available online 8 February 2018

Keywords:
Encaustic
Punic wax
GC–MS
FTIR
TGA
XRD

ABSTRACT

The composition of the ancient wax-based painting technique known as encaustic has long been the subject of debate. Ancient sources provide few details of the technology, and modern understanding of the medium is restricted to theoretical interpretation and experimental observation. In this multi-analytical collaborative study, a number of analytical approaches were used to investigate the physical and molecular properties of a range of experimentally prepared encaustic paints before and after ageing. Analysis using gas chromatography mass spectrometry, Fourier transform infrared spectroscopy (invasive and non-invasive), X-ray diffraction and thermogravimetric analysis demonstrated how differences in the technology of production alter the properties and composition of the medium and showed how these are modified by the addition of pigment and the effects of ageing. Comparison of results from the different analytical techniques highlights the benefit of an integrated analytical approach to the analysis of ancient encaustic paints and the fundamental importance of insights from invasive study to evaluating the results of non-invasive analysis.

1. Introduction

The wax-based painting technique, known as encaustic, was used in antiquity for the production of wall and panel paintings (such as the Roman period Egyptian mummy portraits), ceramics and polychrome sculpture [1]. The ancient documentary sources provide few details of the technology of the technique, which has been a subject of much debate for many years [1,2]. In consequence, modern understanding of the medium is limited to theoretical interpretation of the results obtained from analysis of ancient encaustic paints and observations from experimental reproduction, either to replicate ancient recipes, model the interpretation of analytical studies or to explore working properties [1,3,4].

The controversy surrounding the interpretation of the ancient medium of encaustic centres on the working properties of the wax. Two approaches to employ the medium are possible: a 'hot' technique, in which the wax is applied in a molten state, and a "cold" technique, in which it is applied as an emulsion after modification of the wax by alkali saponification or addition of soap. The latter has garnered much support, as it is consistent with evidence for brush work often observed on encaustic painted surfaces and performs well in replication experiments [5]. It has also been argued that Pliny's description of the preparation of "Punic wax" from beeswax can be interpreted as an emulsified wax product [3,4], although an alternative interpretation of 'Punic wax' as a clarified version of beeswax is more consistent with Pliny's account [6,7].

Analytical studies of ancient paints appear to support the 'cold' encaustic emulsion theory, as fatty acid soaps are invariably encountered during analysis [1,3,8–10]. However, the formation of soaps via pigment-medium interactions is frequently observed in lipid-bound paint systems [11–13] and experimental approaches to date have not attempted to model the extent to which ageing might mimic or conceal the analytical evidence for wax processing.

In this study a number of analytical approaches were used to investigate this problem, comparing the physical and molecular properties of a range of experimentally prepared encaustic paints before and after ageing. The work was undertaken within the framework of the EU consortium IPERION-CH, enabling the collaboration of six research teams and the application and evaluation of a range of approaches to

* Corresponding author.
E-mail address: rstacey@thebritishmuseum.ac.uk (R.J. Stacey).

https://doi.org/10.1016/j.microc.2018.01.040

conventional diagnostic analysis compared with non-invasive analytical methods.

The aims of the investigation were threefold:

1) To understand how differences in the technology of production alter the properties and composition of the medium.
2) To determine how chemical markers for differences in composition of different encaustic media are modified by the addition of pigment and the effects of ageing.
3) To compare and evaluate which analytical techniques are most suited to this purpose and how invasive sampling and analysis can inform the interpretation of results acquired non-invasively.

Addressing these questions is fundamental to understanding the technology of ancient encaustic media, which in turn informs the understanding of painting technique and the Classical accounts of the manufacturing technology and raw materials. It is equally vital to understand how well both our established and emerging analytical technologies perform as tools to probe these questions and how we can best direct these approaches towards future research of ancient encaustic painted surfaces.

For the purpose of these investigations, four different recipes to produce the media were selected. To assess the role of pigment in the ageing behaviour of the medium, one pigment, red lead, has initially been chosen, with a view to extending this selection in future work. The selection was based on the well-established reactivity of lead-based pigments with lipid-based binders. In addition, although lead white is more commonly used in encaustic painting, it was envisaged that in the context of this investigation the highly coloured nature of the red lead pigment would make any pigment decomposition more easily perceptible. The use of red lead in this region at this period has been attested for example by the paint saucers excavated by Petrie at Hawara [14].

2. Materials and methods

2.1. Sample preparation

Four model materials were prepared according to the following recipes:

Recipe 1 (R1) – Pure beeswax untreated: Untreated pure beeswax (Allbäck, used as purchased from Old House Store).

Recipe 2 (R2) – Punic wax: 150 g Pure Beeswax (Allbäck, used as purchased - see above) boiled repeatedly in artificial 'seawater' prepared using 42 g sodium chloride (S7653 from Sigma-Aldrich, UK) in 1200 mL water with 30 g of sodium bicarbonate (S5761 from Sigma-Aldrich, UK). The white waxy material collecting at the surface was skimmed and then washed three times by boiling in 1200 mL deionised water [6].

Recipe 3 (R3) – Alkali-treated wax: 100 mL deionised water, 100 g pure beeswax (Allbäck, used as purchased - see above), 5 g sodium bicarbonate (S5761 from Sigma-Aldrich, UK). Heated together and stirred with no skimming until the wax melts and emulsifies [1].

Recipe 4 (R4) – Pure beeswax with added fatty acids (linseed oil soap): 110 mL deionised water, 111.5 g pure beeswax (Allbäck, used as purchased - see above), 28.8 g linseed oil soap (15–45% soap in water, Allbäck, used as purchased from Old House Store). Heated together and stirred until the wax melts and emulsifies [1]. The purchased linseed oil soap was described as containing sodium salts of mainly natural triglycerides from oleic, linoleic, palmitic acid, linolenic acid and stearic acid. This was confirmed by characterisation of the material, which in addition also showed the presence of some potassium salts.

Each material was then divided into two parts and 5 g red lead (lead (II,IV) oxide, 42,500 from Kremer Pigmente, Germany) pigment was added to one half of each recipe, so that each had a pigmented (WP) and unpigmented (NP) variant. The resulting eight materials were dispersed onto glass slides, using heat and/or a metal spatula as required, in order to obtain a workable material.

The slides were prepared in duplicate to permit two further categories; unaged (UA) and aged (A). The latter were subjected to an ageing regime that combined light and thermal ageing using an Atlas SC340 Solar simulator chamber for a total of 2019 h @ 0.027 Mlux; UV 4.2 μW/lm; RH 60%; T 50 °C. The chamber uses metal halide lamps to simulate solar radiation, with a spectral distribution between 280 and 3000 nm and an irradiance of 1000 W/m^2. The output was filtered using a 5 mm LEXAN filter (a clear solid sheet with light transmission values of 75–87%, depending upon the thickness of sheet but it is essentially opaque to all wavelengths below 385 nm) and Sun-X MT20 film polycarbonate sheet (a museum-grade ultraviolet filter suitable for both internal and external use, which reduces lux levels by 80%, virtually eliminates UV radiation and reduces Solar Heat Gain by 61%).

Ten replicate sets of the final sixteen samples were prepared for distribution to the project participants. Fig. 1 shows a complete and representative set of the final sixteen samples.

2.2. Sample characterisation

2.2.1. Colorimetric measurements and diffuse reflectance spectroscopy

Colorimetric measurements of each sample were carried out to compare the appearance of the media arising from the different recipes and to document colour changes upon ageing. Diffuse reflectance spectra in the visible range and respective colorimetric measurements were acquired by means of the portable spectrophotometer MINOLTA CM2002 equipped with an integration sphere. The measurement area (spot size) is of 4 mm diameter, the spectral range 400–700 nm with a spectral resolution of 10 nm.

2.2.2. Thermogravimetric analysis (TGA)

Thermogravimetric analysis was employed to provide insight into the physical properties of the media and paint films produced by the different recipes and relate these to the working properties observed. The thermal analyses were accomplished under purified N_2 gas at a flow rate of 25 mL/min. A TA Instruments Thermobalance model Q5000IR was used. Measurements were performed at a rate of 10 °C/min, from 30 °C to 900 °C. The amount of sample in each TGA measurement varied between 2 and 4 mg.

2.2.3. X-ray diffraction

X-ray diffraction analysis was carried out using a PANalyticaldiffractometerX'Pert PRO with radiation CuKα1 = 1.54 Å, operating at 40 kV, 30 mA, 2θ range 3–70° step size 0.02°, time per step 50 s, equipped with X'Celerator RTMS (Real Time Multiple Strip) X-ray detection technology and High Score data acquisition and interpretation software. A zero background sample holder was used.

2.2.4. GC–MS

Molecular analysis of the samples using gas chromatography mass spectrometry (GC–MS) was carried out at three institutions, using five different sample preparation protocols. The analytical procedures used in each case were broadly similar and are all based on previously published methods, see Table 1.

The sample preparation protocols were selected to examine the behaviour of components of the beeswax in response to the processing involved in the recipes, the presence of pigment and the effects of ageing. The fate of free fatty acids, fatty acids soaps and alkyl wax esters was of particular interest and the five methods allowed changes to these to be compared in different ways:

Protocol 1 (a) Microwave assisted saponification (10 wt% KOH in EtOH) followed by multiple solvent extractions and silylation using BSTFA + TMCS (1%). By this procedure the alkyl wax esters are hydrolysed and all free fatty acids and fatty acid salts are silylated [15]; (b) aqueous extraction of carboxylate salts followed by diethyl ether extraction of the acidified solution and silylation using BSTFA + TMCS (1%). By this procedure the fatty acid soaps are isolated [2].

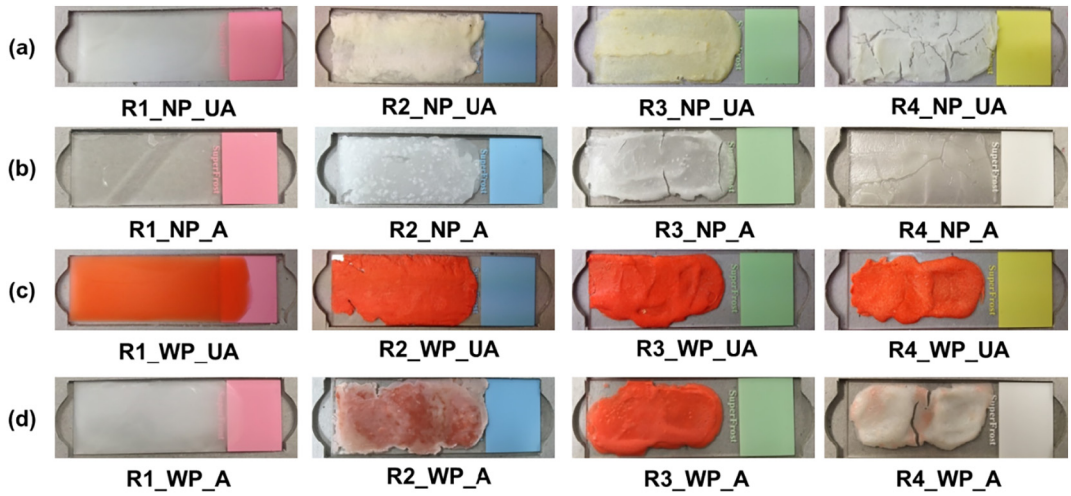

Fig. 1. Representative set of the final sixteen samples produced from the four recipes; Recipe 1 (R1) – pure beeswax, untreated; Recipe 2 (R2) –Punic wax; Recipe 3 (R3) – Alkali-treated wax; Recipe 4 (R4) – Pure beeswax with added linseed oil soap: (a) with no pigment (NP), unaged (UA); (b) with no pigment (NP), aged (A); (c) with pigment (WP), unaged (UA) and (d) with pigment (WP), aged (A).

Protocol 2 (a & b) Solvent extraction with dichloromethane followed, after division of the sample into two aliquots, by; (a) silylation using BSTFA + TMCS (1%) and (b) methylation using diazomethane. In both (a) and (b) the alkyl wax esters remain intact; in (a) free fatty acids and fatty acid salts are silylated, in (b) only the free fatty acids are methylated.

Protocol 3 Solvent extraction followed by butylation using butanolic Methprep II. Meth-Prep II, a commonly used transesterification reagent contains methanol that reacts with esters to produce alcohol and palmitic acid. Replacing the methanol with the tertiary alcohol t-butanol prevents transesterification [16]. The alkyl wax esters remain intact and the free fatty acids and fatty acid salts are butylated.

2.2.5. FTIR

FTIR spectra in macro ATR mode were recorded using a Thermo Nicolet Nexus 5700 spectrometer with a solid-substrate beamsplitter. The ATR spectra were registered by means of a diamond ATR Smart Orbit™ accessory with a spectral resolution of 4 cm^{-1} and 64 scans are recorded in the 4000–400 cm^{-1} range. A small amount of wax was sampled from the glass slides and applied directly onto the ATR crystal.

Non-invasive reflection FTIR study was performed by the Bruker ALPHA spectrometer equipped with a specific module for reflection-mode measurements through a system of parabolic mirrors allowing the infrared radiation to be sent and collected (22°/22°). The sample-probe distance is about 1 cm and 250 scans are recorded in the 8000–400 cm^{-1} range. The spatial resolution is of 28 mm^2. Whenever possible, three points were measured for each sample in order to evaluate the reproducibility of the measurements and the homogeneity of the sample.

3. Results and discussion

3.1. Molecular characterisation of the four recipes

3.1.1. GC–MS

The typical beeswax composition expected from samples of the unpigmented and unaged films of R1 (Fig. 2) was observed by all protocols. Thus, long-chain fatty acids with an even number of carbons (from C16 to C34), long-chain *n*-alcohols with an even number of carbons (from C24 to C34, peaking at C30) and long-chain odd carbon number *n*-alkanes (from C21 to C33) were seen. In Protocol 1a higher relative abundance of *n*-alcohols and C16 fatty acids was observed, reflecting the generation of these compounds by hydrolysis of the alkyl wax esters, as well as even-chain length (ω-1)-hydroxy acids and (α,ω-1)-diols from the hydroxy wax esters. The typical beeswax palmitate wax esters (from C40 to C50) and corresponding hydroxyl wax esters were seen by Protocols 2 and 3. In addition, three unexpected steryl esters were observed in abundance by Protocols 2 and 3, indicating contamination or adulteration

Table 1
Summary of GC–MS parameters used for sample analysis after different preparation protocols. Institution where analysis was carried indicated as follows: Università di Pisa [Pisa]; The British Museum [BM]; The Getty Conservation Institute [GCI].

	Protocol 1 [Pisa]	Protocol 2 [BM]	Protocol 3 [GCI]
Instrument	Agilent 6890N GC Agilent 5973 MS	Agilent 6890N GC Agilent 5975C MS	Agilent 6890N GC Agilent 5975C MS
Injection	PTV in splitless mode at 300 °C	On-column at 50 °C	Splitless injection 280 °C
Carrier gas	Helium. Constant flow at 1.2 ml/min	Helium. Constant flow at 1.5 ml/min	Helium 1 ml/min
Column	J&W HP-5MS 30 m × 0.25 mm, 0.25 μm film thickness with 2 m × 0.32 μm deactivated silica pre-column.	SGE HT-5 12 m × 0.2 mm, 0.1 μm film thickness with 1 m × 0.53 μm retention gap.	25 M × 0.2 mm × 0.2 μm DB-5HT
Oven	80 °C isothermal for 2 min, 10 °C/min up to 200 °C, 200 °C isothermal for 3 min, 10 °C/min up to 280 °C, 280 °C isothermal for 3 min, 20 °C/min up to 300 °C isothermal for 30 min	370 °C at 10 °C/min, after a 1 min isothermal hold at 50 °C with the final temperature held for 15 min.	80 °C (2 min), 10 °C/min to 340 °C (12 min); 20 °C/min to 360 °C (5 min).
MS zones	Interface 280 °C Source 230 °C Quadrupole 180° C Electron impact (EI) positive mode (70 eV)	Interface 350 °C Source 230 °C Quadrupole 150 °C	Interface 300 °C Source 230 °C Quadrupole 150 °C
Acquisition	Scan mode (50–800 amu/s) Solvent delay of 6 min	Scan mode (50–750 amu/s). Solvent delay of 5 min	Scan mode (45–550 amu/s). Solvent delay of 5 min
Ref	Bonaduce et al. [15] Andreotti et al. [2]	Stacey [6]	Mazurek [17] Schilling [18]

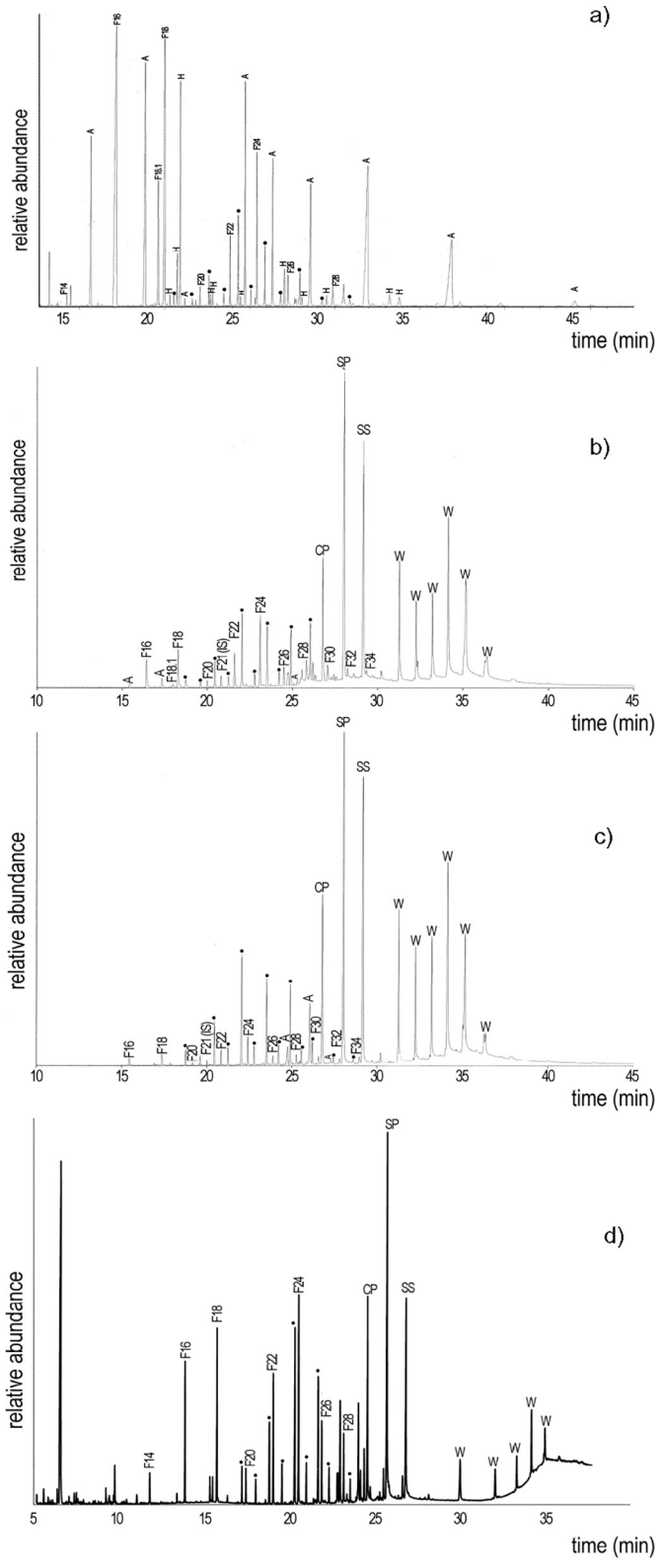

Fig. 2. Partial total ion chromatograms obtained for sample R1_NP_UA (recipe 1, no pigment, unaged) by different GC–MS protocols: (a) Protocol 1a; (b) Protocol 2a; (c) Protocol 2b; (d) Protocol 3. Peak labels: Fn – fatty acid with carbon chain length n; A – n-alkanol; W – wax ester; ● - n-alkane; CP/SP/SS – palmityl palmitate/steryl palmitate/steryl sterate; IS – internal standard.

of the of the beeswax starting material prior to purchase. The unusual (for beeswax) abundance of C18 fatty acid and of C16 and C18 alcohols can also therefore be attributed to this source.

No significant differences between the samples of the unpigmented and unaged films produced from the four recipes were observed by Protocols 1a, 2a and 3, either in the qualitative composition or the relative abundance of components, excepting increased contribution of C16, C18 and, especially, C18:1 fatty acid in R4, due to the presence of the linseed oil soap, although the unsaturated fatty acids were not observed by Protocol 1a&b. Analysis by Protocol 2b (Fig. 3), however, showed a clear

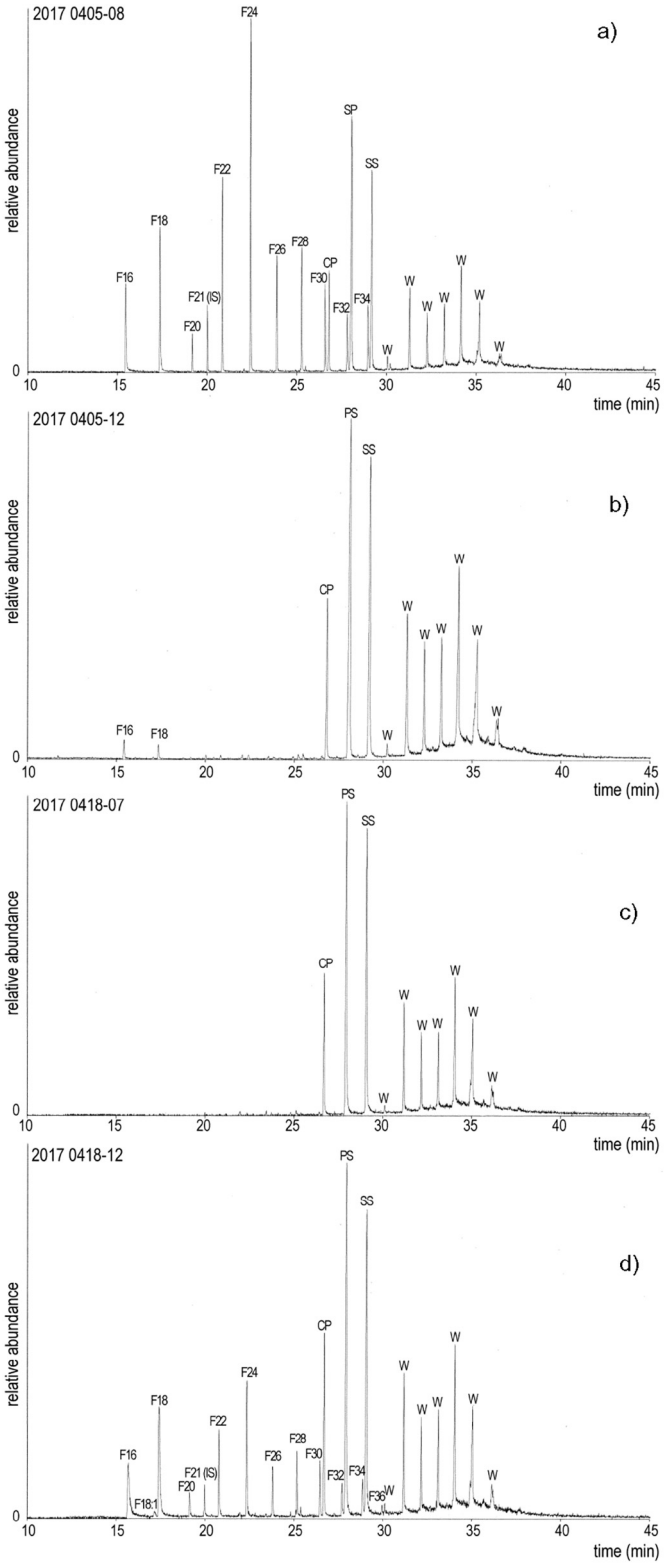

Fig. 3. Partial total ion chromatograms obtained for samples R1-4 (no pigment unaged), obtained using Protocol 2b. Peak labels as for Fig. 2.

difference as R1 and R4 contained abundant free fatty acids (as methyl ester derivatives) which were not detected in R2 and R3 (excepting low levels of C16 and C18). This indicates that the fatty acids have been fully saponified by the processing in these recipes. The low levels of oleic acid detected in R4 by Protocol 2b imply that minimal free fatty acids are contributed by the linseed oil soap.

The recovery and analysis of fatty acid salts by Protocol 1b allows the degree of saponification occurring during preparation of the recipes to be evaluated further. Fig. 4 shows palmitic acid (C16:0), stearic acid (C18:0) and hydroxy acids (14-hydroxy hexadecanoic acid and 15-hydroxy hexadecanoic acid) detected in R2 and R3 by this protocol compared with their effective absence (equivalent to laboratory blank levels) in the unprocessed beeswax of R1. These results are in agreement with a partial saponification of the wax monoesters and hydroxyesters that took place during the treatment of beeswax with sodium bicarbonate to obtain Punic wax. The ratio between the total abundance of hydroxy fatty acids and that of palmitic acid (Σ OHC_{16}/C_{16}), calculated as the area of the hydroxy acids respect to that of palmitic acid was of 0.1–0.3 in agreement with the literature that reports values between 0.1 and 7.2 [2]. Values are not modified by the ageing for R1 and R3.

By Protocol 2b changes taking place on addition of pigment can be observed (Fig. 5): the free fatty acids originally present in R4 are absent after pigment is added. It is notable that the same phenomenon is not seen in R1, implying that interaction of the free fatty acids with the pigment to form metal salts is promoted by the prior presence of soaps and occurs immediately when the pigment is incorporated without the need for ageing.

3.1.2. FTIR

The spectra of samples taken from an unaged and unpigmented film of R1 show the now well-characterized bands for beeswax [1,3,19], namely;

a) the stretching vibrations of the alcohol hydroxy groups at 3450–3200 cm^{-1};
b) a doublet at 2916 and 2848 cm^{-1}, the symmetric and antisymmetric stretching vibrations of the CH_2 groups;
c) the carbonyl band of esters at about 1734 cm^{-1};
d) weak and sharp bands at 1709 and 1693 cm^{-1}, due to the carbonyl groups of un-ionized carboxyls of organic acids;
e) the doublet at 1472 and 1462 cm^{-1} due to the planar deformation vibrations (or scissoring) of CH_2 groups, together with the doublet at 730 and 719 cm^{-1} (see below), these indicate an ordered orthorhombic packing of the long aliphatic chains [20,21];
f) the range 1300–1100 cm^{-1}, including the stretching vibrations of C-O-C groups at about 1170 cm^{-1} and the CH_2 wagging and twisting modes. The range also includes the C-C-C skeletal vibration modes of the chain.
g) the set of bands observed between 1000 and 720 cm^{-1}, assigned to the rocking modes of the methylene chains, with the most intense doublet at 730 and 719 cm^{-1} assigned to nonplanar skeletal

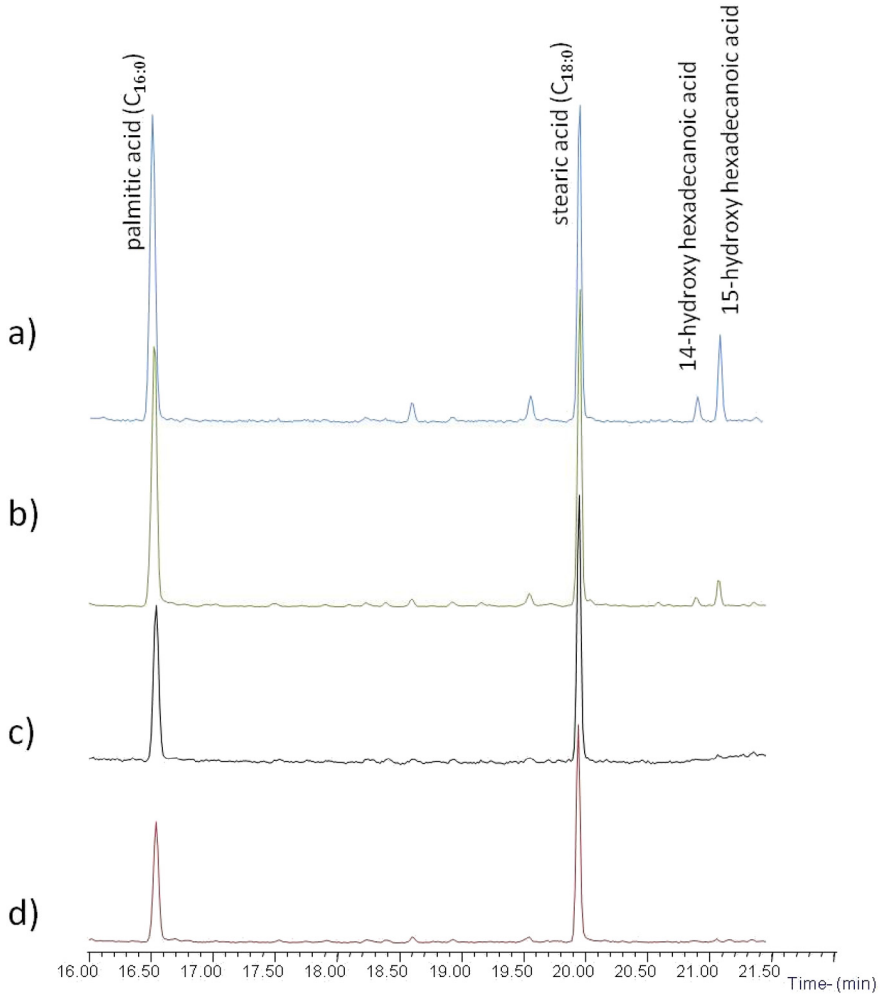

Fig. 4. TIC chromatograms of the aqueous extracted a) R2-np-ua; b) R3-np-ua; c) R4-np-ua; d) R1-np-ua; c) d) without pigment and unaged analysed by GC/MS.

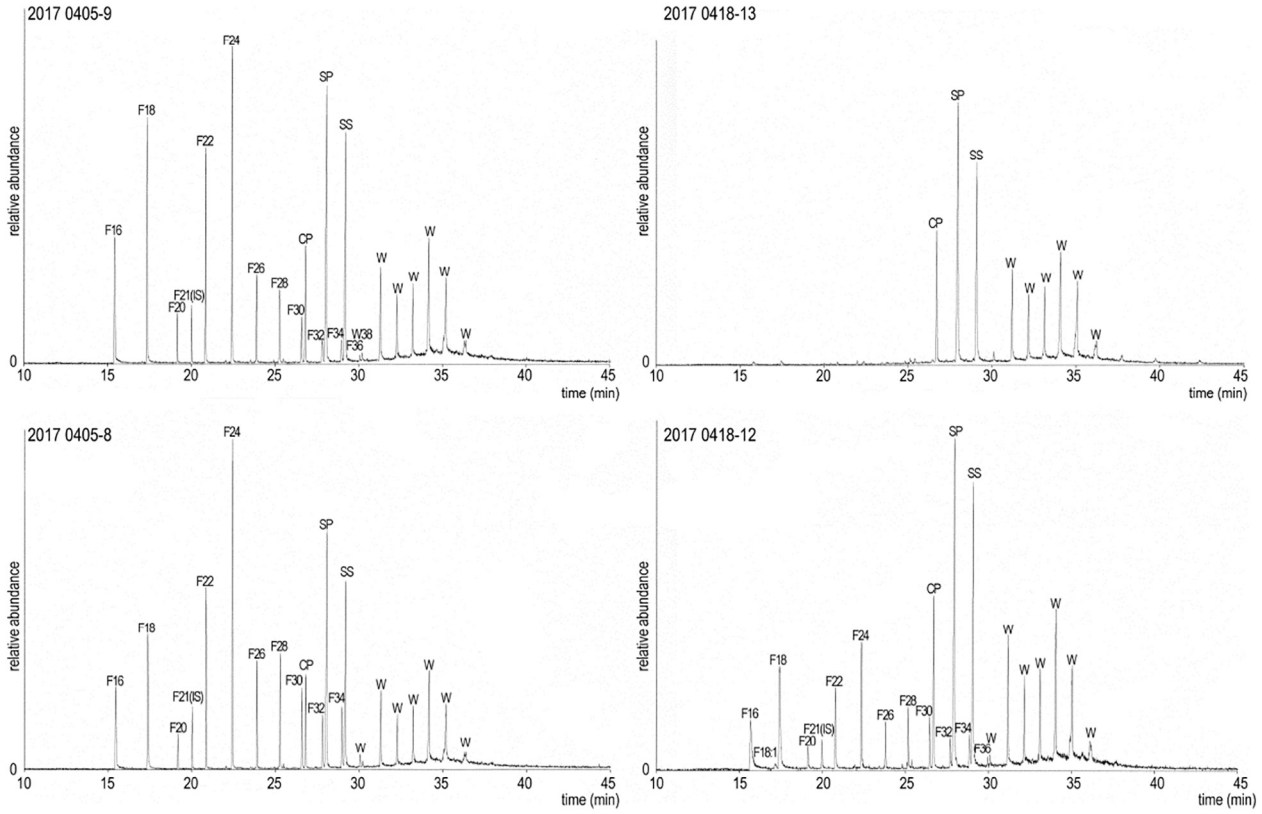

Fig. 5. Partial total ion chromatograms obtained for samples R1 (left) and R4 (right) with (top) and without (bottom) pigment. Peak labels as for Fig. 2.

deformation vibrations of long-chain hydrocarbons. The band at 890 cm^{-1} is also assigned to the rocking motion of CH_3 group.

Some of these features are presented in Fig. 6(a) (R1_NP_UA) where the spectral region 1800–650 cm^{-1} has been selected to enhance the visibility of change with pigment and ageing. On addition of the red lead pigment small changes are observed in the spectra (Fig. 6(a); R1_WP_UA), most notably a small decrease in the bands at 1709 and 1693 cm^{-1}, and the appearance of a band at 1511 cm^{-1}. These observations are consistent with the production of lead fatty acid soaps. Evidence of soap formation is also observed in the spectra of samples from the unaged and unpigmented films of R2 (Fig. 6(b); R2_NP_UA) and R3 (Fig. 6(c); R3_NP_UA). Thus, the bands at 1709 and 1693 cm^{-1}, as seen in the pure beeswax sample, have almost disappeared and a sharp band at 1555 cm^{-1} is observed. This is assigned to the antisymmetric stretch of a sodium carboxylate, likely formed as a result of the preparation procedure employed [22].

The spectra of samples from the unaged and unpigmented films of R4 (Fig. 6(d); R4_NP_UA) appear very similar to those of R1 (Fig. 6(a); R1_NP_UA), with no evidence for the bands of the added linseed oil soap. On addition of pigment two bands typical of lead carboxylates at 1539 and 1511 cm^{-1} are evident in the spectra (Fig. 6(d); R4_WP_UA), together with a band at 1562 cm^{-1}, reminiscent of the sodium carboxylate observed in samples R2 and R3, but with the sodium deriving from the added oil soap rather than from the wax processing.

3.1.3. Thermogravimetric analysis

Thermogravimetric analysis (TGA) provided insights into the physical properties of the four encaustic media. When interpreted alongside the FTIR and GC–MS results these offer further indications of species formed as a result of preparation procedures and their significance for appearance and working properties.

Fig. 7 shows the differential thermogravimetric (DTG) curves obtained for the different paint model systems analysed. The experimental temperatures and the percentage mass losses of the corresponding thermal degradation steps are summarized in Table 2.

The pyrolysis of beeswax is characterized by a broad mass loss in the range 200–250 °C, followed by a mass loss with a maximum in the DTG curve at 306 °C. The first mass loss is due to the evaporation of the *n*-alkanes and the hydroxyl fatty acids in the beeswax. The second mass loss can be attributed to the lipid fraction [23].

Prior to ageing the DTG curve of samples from a film of R1 without pigment (Fig. 7(a)) is in agreement with a reference sample of beeswax, however the mass losses are observed to occur at slightly higher temperature (Table 2), pointing to an increase of the thermal stability of the wax, perhaps due to the heating process for its application. The DTG curves of samples from the unpigmented films of R2, R3 and R4 (Fig. 7(a)) also showed a similar profile, plus a mass loss in the range 430–470 °C (Table 2). For R2 and R3, this mass loss (8–12%) seems to be associated with the sodium carboxylates generated in the preparation process, as observed from the FTIR data. The curves of metal soaps of oils in the literature showed a multi-stage process characterized by an abrupt mass loss above 40% between 400 and 500 °C. A residue of 10–50% is reported depending on the metal [24,25]. A slightly higher amount of sodium carboxylates in R3, resulting directly from the formation of an emulsion during the preparation, is in agreement with the presence of a residue (1%) at 800 °C. R4 shows the presence of a small mass loss (around 3%) at 500 °C related to the linseed oil soaps added. This percentage is in agreement with the low amount of soaps added to the recipe. The oil soap product is described by the manufacturer as containing 15–45% soap, but analysis of the product (not presented here) suggests the actual concentration could be as little as 9%. Since the oil soap product contributes only 26% *w*/w of the R4 recipe, the linseed oil soap content could be as little as 3%. This perhaps explains

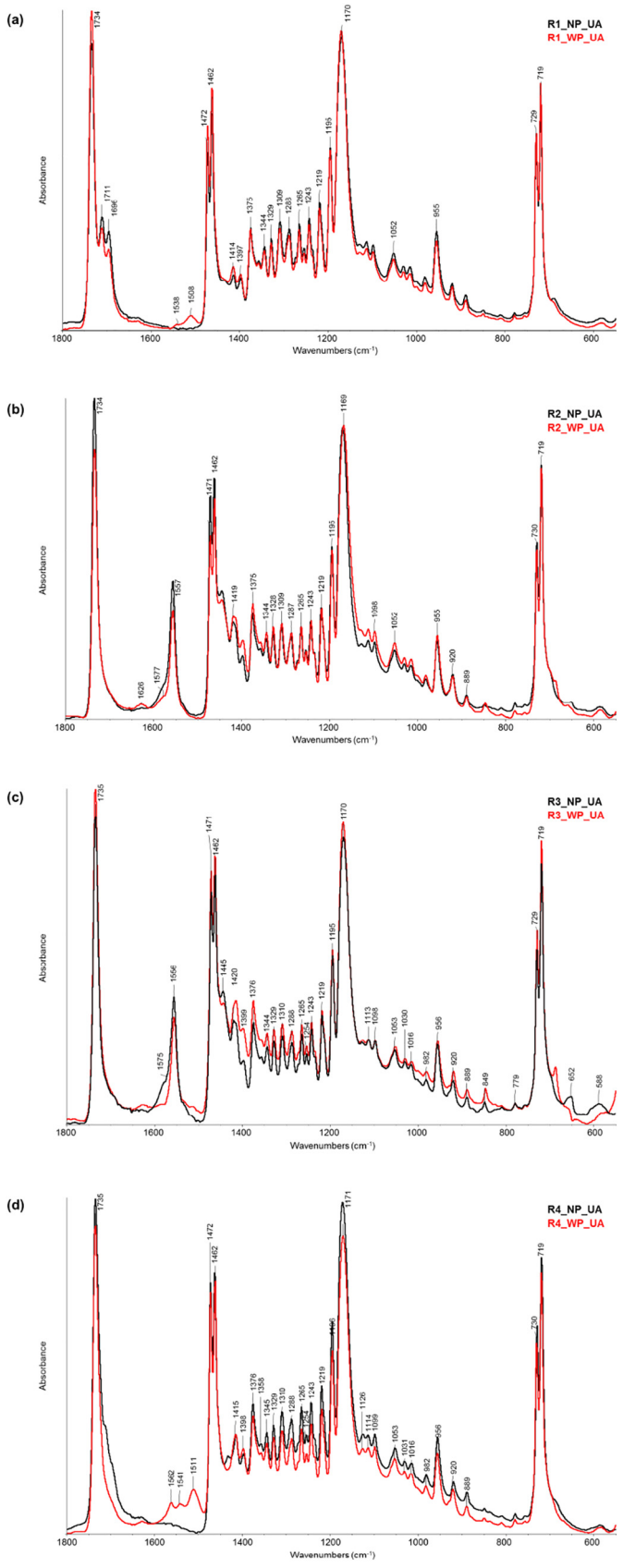

Fig. 6. FTIR spectra in macro ATR mode of: (a) Recipe 1 (R1) – pure beeswax, untreated; (b) Recipe 2 (R2) –Punic wax; (c) Recipe 3 (R3) – Alkali-treated wax; (d) Recipe 4 (R4) – Pure beeswax with added linseed oil soap; with no pigment (NP, black), and with pigment (WP, red), unaged (UA).

the absence of the corresponding signals obtained by other techniques (see FTIR and GC/MS).

The addition of pigment to R1 (Fig. 7(c)) results in a widening of the DTG curves acquired for samples from this film, which exhibits a broad, ill-defined mass loss with a maximum around 350–370 °C (around 93%) plus a mass loss at 450 °C (around 5%, Table 2). The formation of a low amount of lead carboxylates could be a possible explanation, as seen in the FTIR data. The presence of lead carboxylates is highlighted by the FTIR and XRD analyses (see sections 3.1.2. and 3.1.3). A residue at 800 °C of the pigmented systems (1–2%) that seems to be related with the unreacted pigment is present (Table 2).

Samples from the pigmented R2 and R3 films (Fig. 7(c)) show DTG curves characterized by an increased mass loss of the peak at 400–500 °C and the presence of a residue at 800 °C (Table 2). These changes are related to the formation of lead carboxylates due to the reactivity of the wax with the pigment. The mass loss also shows different non-resolved degradation steps probably related to the formation of lead carboxylates from carboxylic acids of different alkyl chain length and/or nature [24], although these are not detected by FTIR. However, the two systems (R2 and R3) show different reactivity. In R2 the mass loss at 500 °C increases by 5% while in R3 it increases by 10%. The residues at 800 °C also differ in agreement with the extent of lead carboxylates formation. This different reactivity is probably related to the presence of the remaining unsaponified wax in R3, where an emulsion was formed. This would allow a major reactivity of the lipid fraction of the wax (weight loss centred at 360 °C) to produce carboxylic acids able to react with the pigment. The maximum temperature of the first mass loss related to the beeswax in fact is shifted from 366 °C to 290 °C.

The formation of carboxylates can also be hypothesized from the addition of pigment to R4. As for the other systems the DTG curve (Fig. 7(c)) is characterized by an increased mass loss of the peak at 400-500 °C and the residue at 800 °C (Table 2) in agreement with the ATR-FTIR data which underline the formation of lead soap.

3.2. Alteration due to ageing

3.2.1. Colour change

Colorimetric data obtained before and after ageing are summarized in Table 3.

Some changes to the unpigmented films were noted after ageing (Fig. 1(b)), most notably R2 and R3 as indicated by the ΔE(D65) values (Table 3). In general, R1 appeared more translucent, whereas R2, R3 and R4, became whiter, losing their initial yellow hues, as shown by the negative shift in Δb*(D65) values (Table 3). In terms of texture, the surface roughness of the R2 films is more evident after ageing and cracks spaced in a rectangular grid were observed in the films of R3. By contrast, the cracks in the films of R4 became less discernible, appearing softened, perhaps due to the action of heat on the medium during the ageing procedure.

After ageing dramatic changes were observed in the appearance of the pigmented films (Fig. 1(d)), with the films of R1 and R4 being most affected. In fact the L*a*b* values (see Table 3) after ageing are similar to those observed for the unpigmented variants of these samples, although R1 is more opaque and R4 has some visible patches of remaining pigment. The loss of the characteristic orange hue of the red lead pigment (diffuse reflectance spectral measurements of the four pigmented films prior to ageing (Fig. 8) showed a typical inflection due to the presence of red lead at 560–570 nm in each case) is described by the negative shifts in the Δa*(D65) and Δb*(D65) values (see Table 3).

The films of R2 also partially faded after ageing and developed a whitish powdery texture at the surface of the sample but pigment is still observed to be present, as is the characteristic (but less sharp) inflection point in the diffuse reflectance spectra (Fig. 8(b)).

Only the films of R3 were relatively unaffected with a ΔE(D65) value of only 1.88, although a change in saturation is suggested by the small

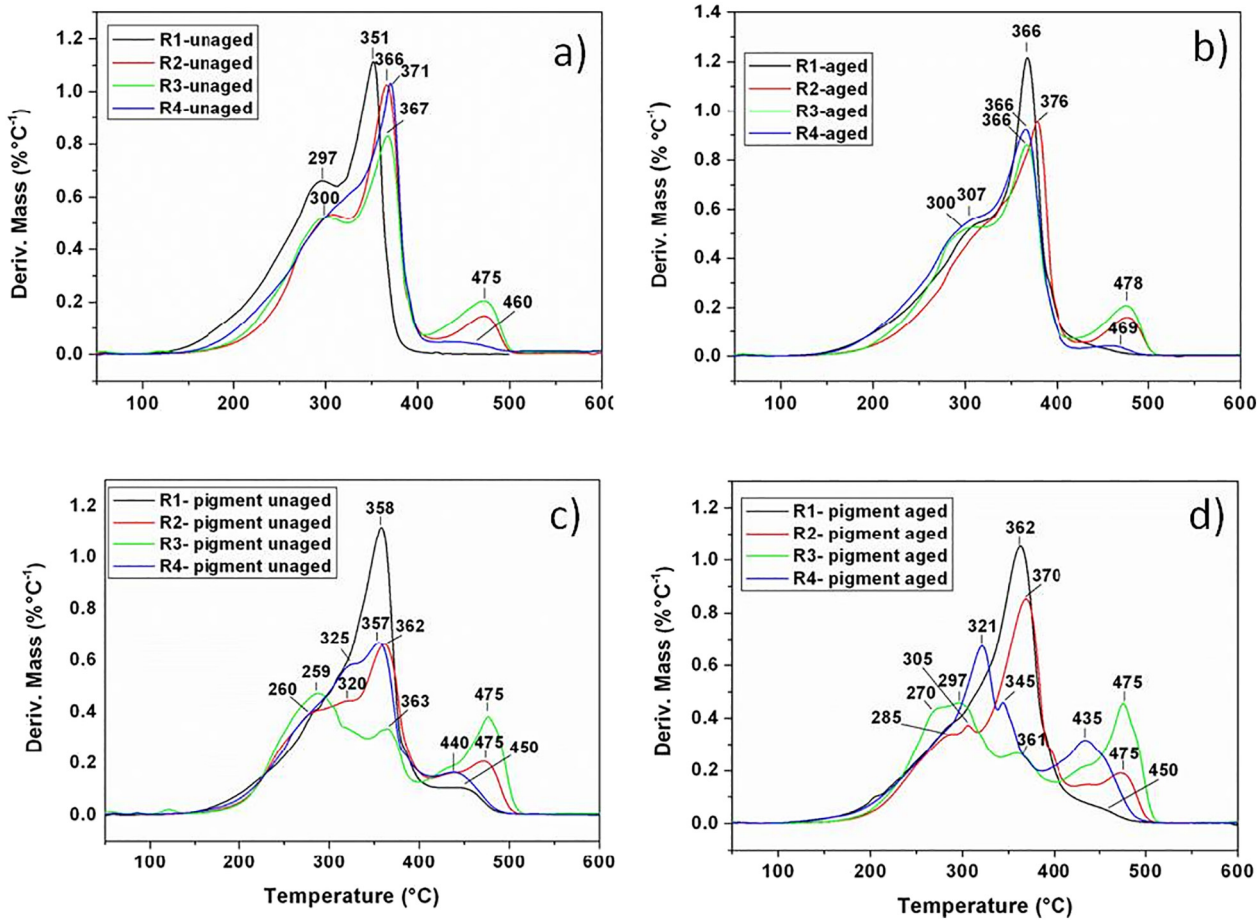

Fig. 7. Difference Thermogravimetric curves under nitrogen, at 10 °C/min for from the four recipes; Recipe 1 (R1) – pure beeswax, untreated; Recipe 2 (R2) –Punic wax; Recipe 3 (R3) – Alkali-treated wax; Recipe 4 (R4) – Pure beeswax with added linseed oil soap: (a) with no pigment (NP), unaged (UA); (b) with no pigment (NP), aged (A); (c) with pigment (WP), unaged (UA) and (d) with pigment (WP), unaged (A).

negative shift in $\Delta C^{**}(D65)$ value = −0.57 (see Table 3, ΔC^* has been calculated as $\Delta C_i^* = C_i^*(A) - C_i^*(UA)$ and $C_i^* = \sqrt{a_i^{*2} + b_i^{*2}}$), perhaps due to the contribution of the medium itself, which in the unpigmented samples (R3_NP_A, Fig. 1 (b)) was shown to whiten, thus adding scattering properties to the paint, upon ageing.

3.2.2. Thermogravimetric analysis

The DTG profiles of the films without pigment (Fig. 7(b)) do not change following ageing, but the decomposition temperatures become slightly higher pointing to a gain of thermal stability. Some hydrolysis of the lipidic part of the beeswax, i.e. diesters to form fatty acids, can be hypothesized on the basis of the loss of definition between the mass losses of the wax.

The ageing of the pigmented system does not seem to modify its thermal behavior. Despite the pronounced colour change (bleaching) observed in the pigmented R1 sample after ageing, the DTG profile does not change substantially (Fig. 7(d)) other than the previously noted slight increase in decomposition temperatures (Table 2). This data, therefore, seems to indicate that the reactivity of the beeswax with the pigment is not dependent on time.

Interestingly, after ageing there is no increase either in the mass loss at 500 °C or in the residue for pigmented R2 and R3 samples, indicating that no changes (in terms of amount of lead carboxylates) occur due to ageing, as observed for R1.

Differently to the other systems, the pigmented R4 sample shows a variation of the mass loss between 400 and 500 °C on ageing but the residue remains unchanged. This would mean that there is no formation of lead carboxylates on ageing but the formation of high molecular weight compounds and polymeric species that show thermal degradation at higher temperatures. This different behaviour could be related to the high reactivity of the linseed oil soap added to the mixture. The high degree of unsaturation of the linseed oil soap, containing mainly salts of linoleic, linolenic and oleic acids, could form a polymerized network or ionomer like system as it dries and ages, as described in the literature [11,27,28].

3.2.3. Molecular alteration

3.2.3.1. GC–MS. Changes to the observed molecular profile after ageing were minimal. In R2 a decrease in the ratio between the total abundance of hydroxy fatty acids and that of palmitic acid (ΣOHC16/ C16) seems to be related to the presence of a higher amount of palmitic acid, pointing to hydrolysis of the material while ageing (Table 2). Interestingly, on ageing, the pigmented R4 sample shows the presence of a lower amount of hydroxyacids that indicate the hydrolysis and formation of metal carboxylates in the sample, as if beeswax showed a higher reactivity in this paint system.

As observed by Protocol 2a, the levels of oleic acid soap in R4 decreased substantially after ageing.

By Protocol 3, a series of odd carbon number long-chain fatty acids (C19, C21 and C23) was observed in all of the aged samples but not detected in the unaged; it is unclear whether these are present as soaps or free fatty acids because they were not detected when other protocols were used.

Table 2
Experimental temperatures and the percentage mass losses of the corresponding degradation steps under nitrogen flow of the four recipes investigated.

	Step no.	NP_UA	WP_UA	NP_A	WP_A
R1	1	297	300	307	306
	2	350 (100%)	358 (94%)	366 (100%)	364 (93%)
	3	–	400–500 (5%)	–	400–500 (5 %)
	Residue at 800 °C	0	1%	0	2%
R2	1	–	270	–	289
	2	308	305 (80%)	313 (86%)	322 (80%)
	3	365 (87%)	368	376	366
	4	472 (9%)	400–500 (15%)	477 (9%)	400–500 (15%)
	5	803 (4%)	803 (5%)	805 (5%)	807 (5%)
	Residue at 800 °C	0	7 %	0	5%
R3	1	52	57	53	53
	2	119	121	–	–
	3	– (86%)	– (68%)	– (87%)	272 (67%)
	4	300	287	300	297
	5	366	366	367	360
	7	471 (13%)	477 (23%)	400–500 (12%)	400–500 (24%)
	Residue at 800 °C	1%	9%	1%	9%
R4	1	300	325	302	321
	2	364 (97%)	356 (78%)	367 (97%)	345 (65%)
	3	449 (3%)	400–500 (10%)	443 (3%)	400–500 (22%)
	Residue at 800 °C	0	12%	0	13%

3.2.3.2. FTIR. The beeswax bands observed for R1 did not appear to be significantly altered following ageing (Fig. 9(a); R1_NP_A). In the pigmented samples (Fig. 9(a); R1_WP_A) a further decrease in the intensity of the bands in the spectra at 1709 and 1693 cm^{-1} is seen and the band at 1511 cm^{-1} increases in intensity and is joined by bands at 1543, 1415 and 1399 cm^{-1}, associated with the antisymmetric and symmetric carboxylate (COO^-) group stretches of the lead soaps. This is consistent with the acceleration in saponification kinetics on both the addition of water and heat to the mixture, as noted by Cotte et al. [29]. In addition the appearance of a small band at *c*.1634 cm^{-1} is observed.

On ageing, bands at 1627 and 1652 cm^{-1} appear in films of R2 and the band at 1555 cm^{-1} broadens and shifts to slightly higher wavelength to 1562 cm^{-1}. Similar behaviour is observed on addition of pigment, except for a change in shape of the band at about 1414 cm^{-1} and the appearance of a band at 1511 cm^{-1} (Fig. 9(b); R2_WP_A), which is related to the formation of lead carboxylates.

Comparable trends are observed in the films of R3 (Fig. 9(c)), where after ageing in both unpigmented and pigmented samples, the shape of the bands due to sodium soap formation, observed in the unaged samples at 1555 cm^{-1} and 1412 cm^{-1} (Fig. 9(c); R3_NP_UA and R3_WP_UA), changes and the band at c.1555 cm^{-1} shifts to 1562 cm^{-1}. A band at 1627 cm^{-1} is also observed to appear (Fig. 9(c); R3_NP_A and R3_WP_A). In the pigmented samples some bands, particularly those at around the 1400 cm^{-1} range, at 848 cm^{-1} and at 688 cm^{-1}, increase on ageing. However, perhaps most interestingly, the bands at 1540 and 1510 cm^{-1}, associated with the formation of lead soaps are not detected in the pigmented samples. This may suggest that, despite the similarities in their FTIR spectra, some differences in R2 and R3 may be used to distinguish these chemically. Their appearance, especially on ageing is very different.

The spectra of samples from unpigmented films of R4 (Fig. 6(d); R4_NP_UA), which prior to ageing, appear very similar to those of R1 (Fig. 6(a); R1_NP_UA), show, after ageing a marked increase in intensity of the bands at 1709 and 1693 cm^{-1} (Fig. 9(d); R4_NP_A), due to the carbonyl groups of un-ionized carboxyls of organic acids. In pigmented films (Fig. 9(d); R4_WP_A), the sodium carboxylate band at 1562 cm^{-1} tends to decrease after ageing, whilst the bands associated with the lead carboxylates at 1511 and 1539 cm^{-1} are observed to increase. Moreover, two bands at 1624 and 1650 cm^{-1} are evident. This may suggest sequestering of free acids, released by wax ester degradation, by the sodium and lead ions "in solution", with lead carboxylates dominating over sodium carboxylates on ageing.

Table 3
Colorimetric data for the sixteen samples. Column headings define standard colour dimensions following Lab colour space conventions, see http://docs-hoffmann.de/cielab03022003.pdf [26].

Sample	L* (D65)	a* (D65)	b* (D65)	ΔE (D65)	ΔL* (D65)	Δa* (D65)	Δb* (D65)
R1_NP_UA	67.91	−1.08	8.68	3.14	1.78	0.35	−2.57
R1_NP_A	69.68	−0.73	6.11				
R2_NP_UA	80.80	−1.80	9.45	15.77	−15.56	0.89	−2.40
R2_NP_A	65.24	−0.92	7.05				
R3_NP_UA	65.76	−1.73	22.81	16.55	3.14	0.94	−16.22
R3_NP_A	68.90	−0.80	6.59				
R4_NP_UA	76.93	−2.49	12.54	9.44	−7.25	2.02	−5.71
R4_NP_A	69.69	−0.47	6.84				
R1_WP_UA	54.87	34.54	42.90	52.85	8.10	−35.05	−38.72
R1_WP_A	62.97	−0.51	4.19				
R2_WP_UA	63.79	41.95	42.73	29.50	−6.93	−18.98	−21.51
R2_WP_A	56.87	22.98	21.22				
R3_WP_UA	54.95	41.77	42.75	1.88	−0.73	0.75	−1.56
R3_WP_A	54.22	42.52	41.19				
R4_WP_UA	60.12	37.24	39.65	45.26	7.45	−33.96	−28.98
R4_WP_A	67.57	3.28	10.68				

3.2.4. X-ray diffraction

The characteristic pattern of beeswax was obtained for all the samples analysed. The pattern is composed of a first region of peaks at 2θ 2,33°, 3,24°, 4,50°, 5,80°, and a second one at 19,45°, 21,6°, 24,00°, 30,00°, 35, 9° corresponding to the monoclinic and orthorhombic structures of beeswax, respectively (Fig. 10(a)). These two distinct regions are attributed in the literature to the diesters and hydrocarbons/monoesters fractions, respectively [27,30,31].

Inorganic compounds were identified in the patterns obtained. The presence of halite (NaCl) was recorded (main peaks at 2θ 31,82° (100), 45,54° (83), 56,40° (33)) for all samples of R2 and for the unpigmented samples of R4; the origin of this is residual from the wax processing or in the case of R4 presumably residual from the linseed oil soap production process. Red lead, added as a pigment, was observed for all the pigmented samples (Fig. 10(b)) except for R1 WP A and R4 WP A, in which all the peaks of red lead (main peaks at 2θ 26,39° (100); 32,14° (45,7), 30,79° (34,6)) are not present. This is in agreement with the complete bleaching observed in these samples upon ageing.

Crystalline metal carboxylates were identified in some of the unpigmented model systems. Recipes R2 and R3, showed the presence of traces of the characteristic peaks of sodium carboxylates of saturated long chain fatty acids, such as sodium stearates, at 2θ 1,49°, 2,28°, 4,05°, 5,69°, 21,57°, 27,54°, 31,85°, 40,66° (Fig. 11(a)). This is in agreement with the sharp carboxylate band observed by FTIR at *c.* 1560 cm^{-1}.

The formation of lead carboxylates was observed only for R1_WP_A, where traces of peaks at 2θ 2,03°, 3,88°, 5,79°, 7,48°, 19,59°, 29,92° seem to be related to lead palmitate [9] (Fig. 11(b)). The patterns of R2 and R3 pigmented systems (both aged and unaged) do not show the presence of crystalline compounds related to metal carboxylates. This could be related to the formation of non-crystalline forms or to the formation of a crystalline fraction that is below the detection limit of the instrument. From FTIR, the band related to lead carboxylates (1511 cm^{-1}) showed a very low absorbance. In fact, the mass loss measured in the range of carboxylates by TGA is below the 10%. However, the modification of the metal carboxylate band at *c.*1560 cm^{-1} (broadening and wavelength shift) occurring in the FTIR spectra of the aged and pigmented samples could be in agreement with the formation of non-

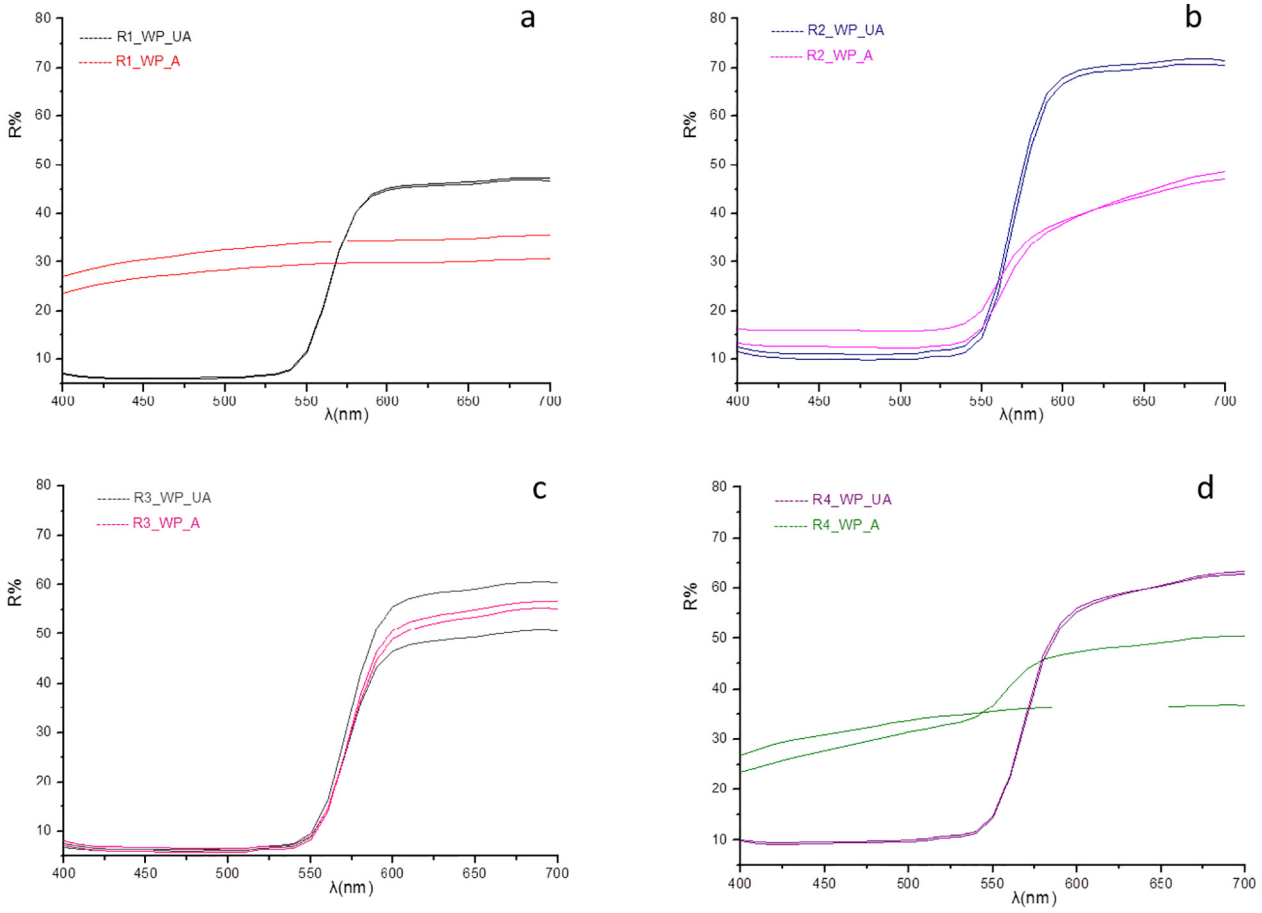

Fig. 8. Diffuse reflectance spectra of (a) Recipe 1 (R1) – pure beeswax, untreated; (b) Recipe 2 (R2) –Punic wax; (c) Recipe 3 (R3) – Alkali-treated wax; (d) Recipe 4 (R4) – Pure beeswax with added linseed oil soap; with pigment (WP), before (UA) and after ageing (A).

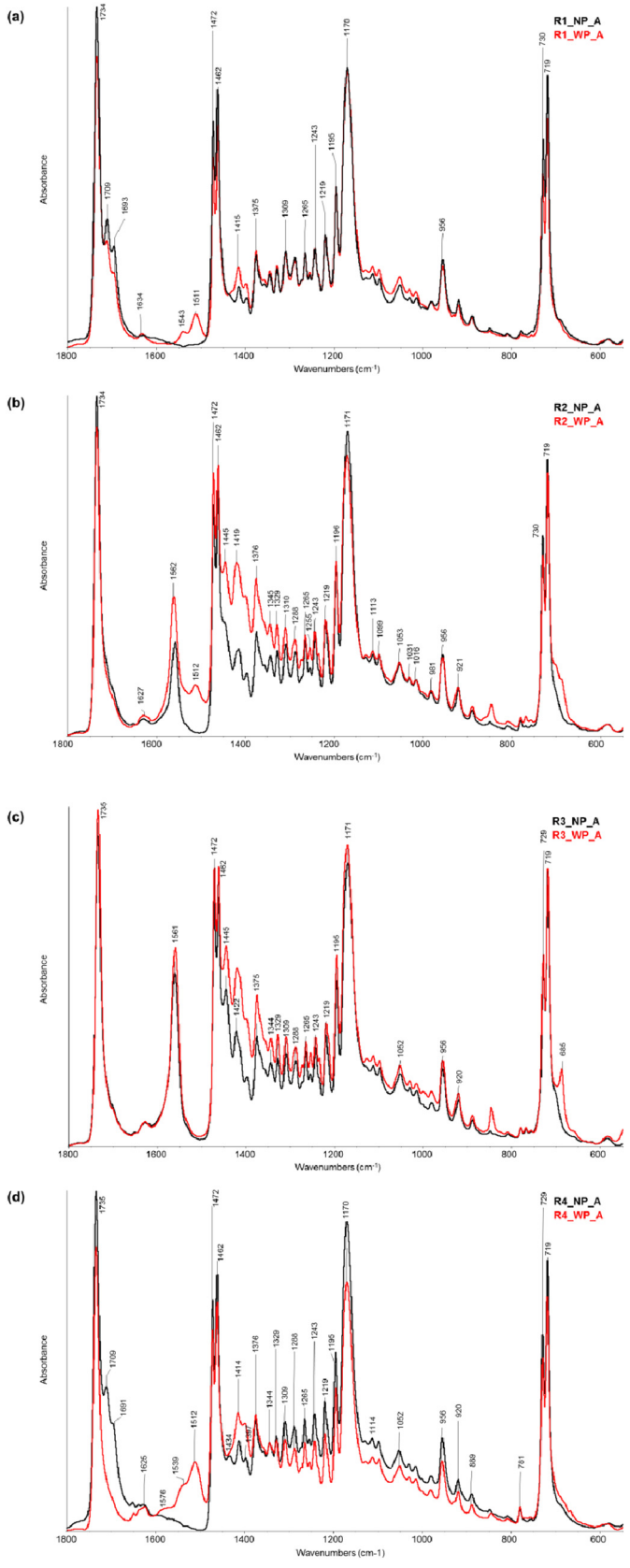

Fig. 9. FTIR spectra in macro ATR mode of: (a) Recipe 1 (R1) – pure beeswax, untreated; (b) Recipe 2 (R2) –Punic wax; (c) Recipe 3 (R3) – Alkali-treated wax; (d) Recipe 4 (R4) – Pure beeswax with added linseed oil soap; with no pigment (NP, black), and with pigment (WP, red), aged (A).

crystalline (disordered) metal complexes, as described in the literature [25,28]. The pattern for the aged sample of R3 with pigment, also showed the presence of further peaks. However, comparison with databases did not allow the crystalline phase(s) to be determined.

The samples of R4 do not show the presence of the linseed oil soap. The amount of material added (as discussed in the TGA section) and the low crystallinity of the reference material justifies a pattern that matches the one of R1_NP_UA (Fig. 10(a)). R4 WP A (Fig. 10(c)), however, shows significant differences with the patterns obtained for the other systems. No peaks related to the presence of red lead were identified and no peaks were registered in the range of 2θ between 0 and 10, attributable to the monoclinic structure of beeswax. The peaks in the pattern obtained are attributable to the orthorhombic structure of hydrocarbons/monoesters fraction of the beeswax and only the peak at 34, 07° could be related to a pure unsaturated fatty acid (see oleic acid pattern in Fig. 10(c)). This could be related to the high reactivity of the linseed oil soap added to the mixture. The high degree of unsaturation of the linseed oil soap can generate a polymer matrix as it dries and ages through autoxidation. The results obtained point to the reaction of the beeswax compounds with the linseed oil soaps during this process in agreement with TGA data, losing crystallinity and gaining molecular weight.

3.3. Implications for properties of the encaustic products and recipe identification

Significant differences were evident from the outset between the different recipes (Fig. 1 (a)) even before addition of the pigment or undergoing ageing. The requirement for different techniques to disperse the films on the glass slides immediately hinted at the very different working properties of each of the media. Thus, the beeswax films (R1), which were applied with minimal direct heating onto the slides, are smooth, white and barely opaque, whereas the other recipes, which required various degrees of heating over a water bath and spreading with a metal spatula to obtain workability of the materials, produced films with thick and uneven textures. In these films agglomerated particles are observed and they appear powdery and slightly yellow with R3 appearing most yellow (see Table 3 for L*a*b* values). In the case of R4, the films also underwent significant shrinkage and cracking following dispersion onto the glass slide. The addition of pigment to the different media also produced varied effects in the four recipes investigated. Prior to ageing (Fig. 1(c)), all the samples appeared similar in hue (see Table 3 for L*a*b* values measured on samples R1-R4_WP_UA), although as with the unpigmented variant, the films of R1 appeared smoother and less opaque than the others. The R2, R3 and R4 films also developed areas of a powdery white bloom after dispersion onto the slides. Some variation in the workability of the media was noted between the pigmented and unpigmented versions of each recipe.

These differences in physical properties are paralleled by differences in the chemical character of the four materials and in their ageing behaviour. The most significant difference is the presence and formation of metal carboxylate soaps. In the unpigmented media R1 contains no soaps whereas R2 and R3 are fully saponified and also exhibit some hydrolysis due to the effects of heating. R4 shows characteristics of both, with FFAs from the unsaponified beeswax and carboxylate soaps from the saponified linseed oil.

When pigment is added, even before ageing has taken place, lead soap formation is observed to some extent in all four encaustic products. In R1 and R4 the lead soaps form by direct saponification of the FFAs in the wax, in R2 and R3 it arises via cation exchange with the sodium soap. The process is increased with ageing and, except in R3,is accompanied by a pronounced loss of colour. The phenomenon is notable because the bleaching of red lead is less commonly observed than its darkening [32]).The few instances of bleaching reported are usually associated either with the formation of sulphates, such as anglesite, $PbSO_4$

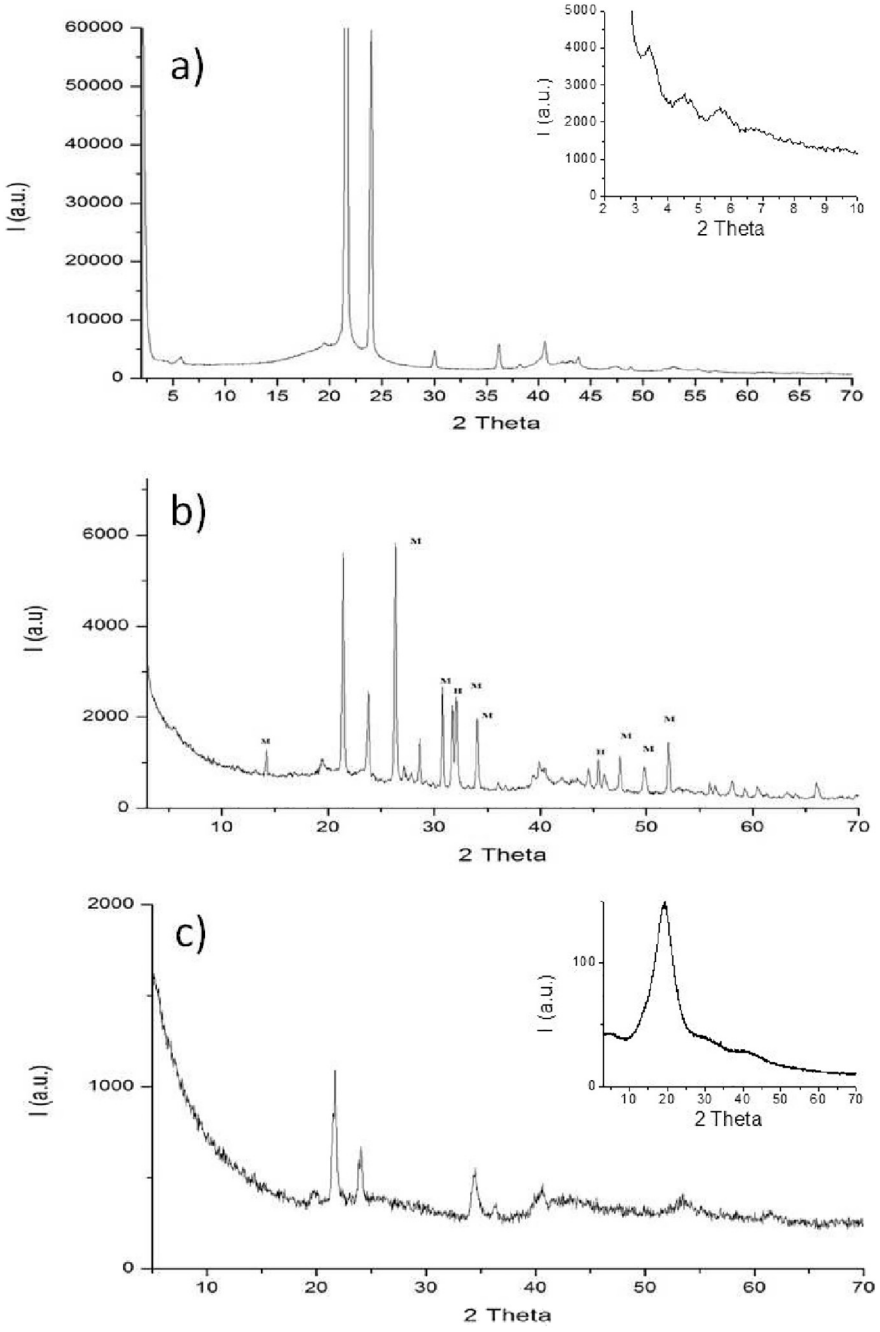

Fig. 10. XRD pattern obtained on a) recipe R1 without pigment and unaged. The first region corresponding to the monoclinic structure of beeswax is highlighted in the zoomed area. b) recipe R2 with pigment unaged (the main peaks of minimum (M) and halite (H) are reported; c) recipe R4 with pigment aged. Oleic acid pattern is provided as an unsaturated fatty acid.

etc. [33], lead carbonates, such as hydrocerussite ($2PbCO_3 \cdot Pb(OH)_2$), cerussite ($PbCO_3$), and plumbonacrite, $Pb_5O(CO_3)_3(OH)_2$ [34–39] or phosgenite, $Pb_2CO_3Cl_2$ [40]. The TGA results from the most completely bleached sample, R1_WP_A show no residue at 800 °C, suggesting complete conversion of red lead to lead carboxylates, while in the other samples unreacted pigment is indicated by residue at 800 °C.

Combined, the evidence from FTIR and TGA indicates that less cation exchange is taking place in R3 than R2 (i.e. higher persistence of sodium soaps and fewer lead soaps) which is perhaps the most distinct difference between these media and is further evidenced by better colour retention in R3 after ageing.

The results therefore present a paradox in terms of medium usability: R1 has the best working properties but the worst colour retention after ageing. It is, however, important to note that only one pigment system has been tested by this study. Different exchange rates or equilibria will operate with other pigment (metal) systems and in real world scenarios of pigment mixtures. Further work to test the workability and stability of the media with different pigments would be worthwhile because the results obtained here imply that an experiential understanding of the medium may be crucial in evaluating the likelihood of different encaustic products being used in antiquity. Sodium carboxylate soaps appear to provide a good indicator for processing of the wax to produce R2 and R3, distinguishing them from R1, but the similarity of R2 and R3 means that no measurable molecular distinction that would differentiate them in a "real world" sample has been observed, especially when the effects of pigmentation and ageing are taken into account.

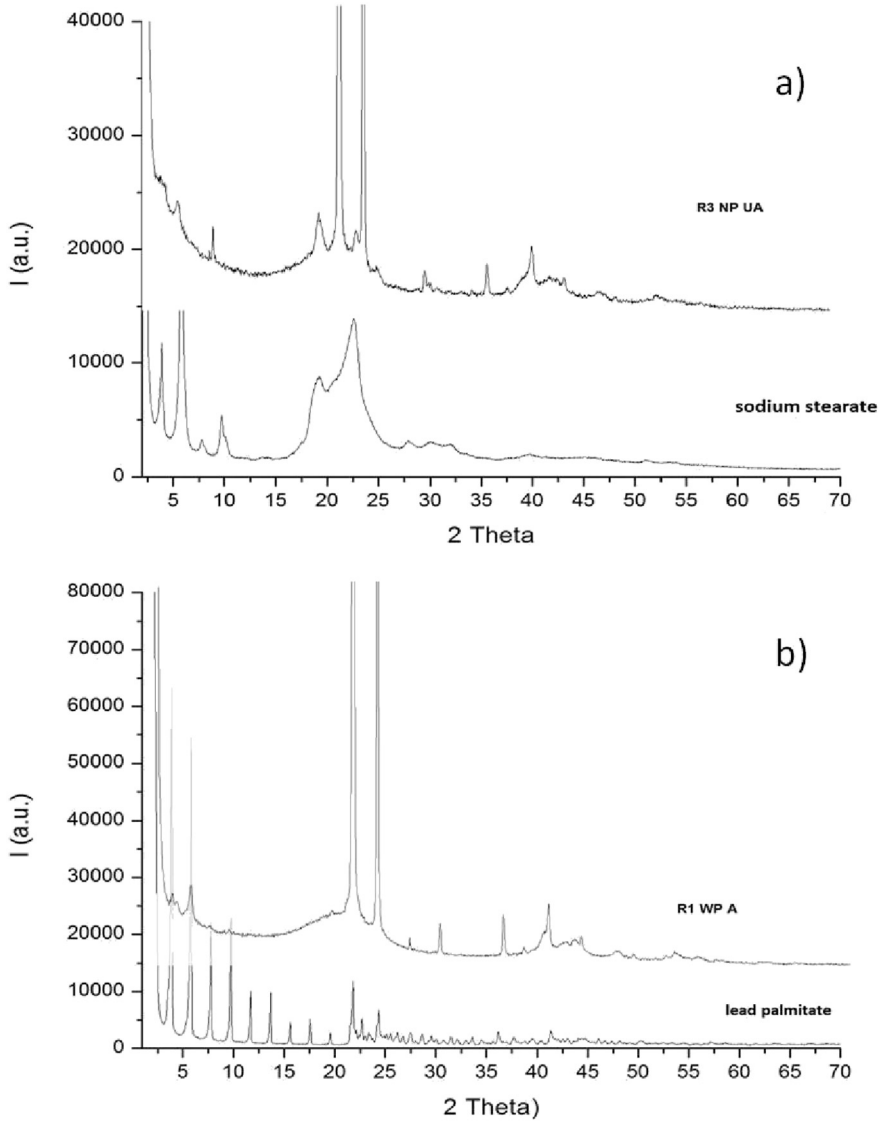

Fig. 11. XRD patterns of a) recipe R3 without pigment aged and unaged versus sodium stearate; b) recipe R1 with pigment aged versus lead palmitate.

3.4. Methodologies compared: assessing the scope for non-invasive studies

3.4.1. Invasive methodologies compared

All the invasive analytical methods produced compositional data sets for the unprocessed beeswax that are comparable to published sources [19,23,41] and reference standards, excepting the detection of an unidentified adulterant wax. This contamination was readily detected by GC–MS analysis, either as unexpected wax esters (Protocols 2a, 2b and 3) or as shorter chain alcohols (C_{16} and C_{18}) derived from their hydrolysis (Protocols 1a and 1b). The ageing behaviour of beeswax has been well-studied; key changes include hydrolysis of wax esters (liberating palmitic acid and long-chain alcohols), loss of free fatty acids in alkaline contexts and sublimation of alkanes in response to heat [42,43] Some of these ageing changes were detected here by FTIR (generation of free fatty acids and alcohols) but interestingly they were not obvious as changed relative abundances in any of the GCMS profiles.

Analysis by GC–MS proved most instructive when the protocol allowed for differentiation of free fatty acids and fatty acid soaps i.e. by comparison of results from Protocols 1b and 2b with those from 1a, 2a and 3. In this way, recipes R2 and R3 could be distinguished by saponification of the free fatty acids in the wax, and soap formation arising from addition of the pigment could be observed. Formation of soaps was indicated by mass losses in the TGA analysis but specific identification of soap species by metal cation was possible only by FTIR and XRD. This information is crucial for determining whether soaps derive from saponification during processing or from pigment medium interaction and this study has revealed the complicated dynamic between carboxylate soaps, free fatty acids released on ageing and metal ions (either from pigment or residual processing salts).

In this experimental study detection of change by comparison of samples has been fundamental to understanding the sample compositions and alterations brought about by processing and ageing, for example, the TGA proved helpful in providing an overview of change in the samples, especially those due to ageing that were not obvious by GC–MS analysis. However, approaches that perform well in a comparison study are not necessarily as instructive when assessing 'real world' samples from ancient painted surfaces, when all processes of medium preparation and alteration with age must be inferred from the one sample. The results presented here show that a combined analytical approach using FTIR, with GC–MS following a protocol that can differentiate soaps and free fatty acids, offers the most potential for detailed molecular characterisation of ancient encaustic paints where sampling is possible.

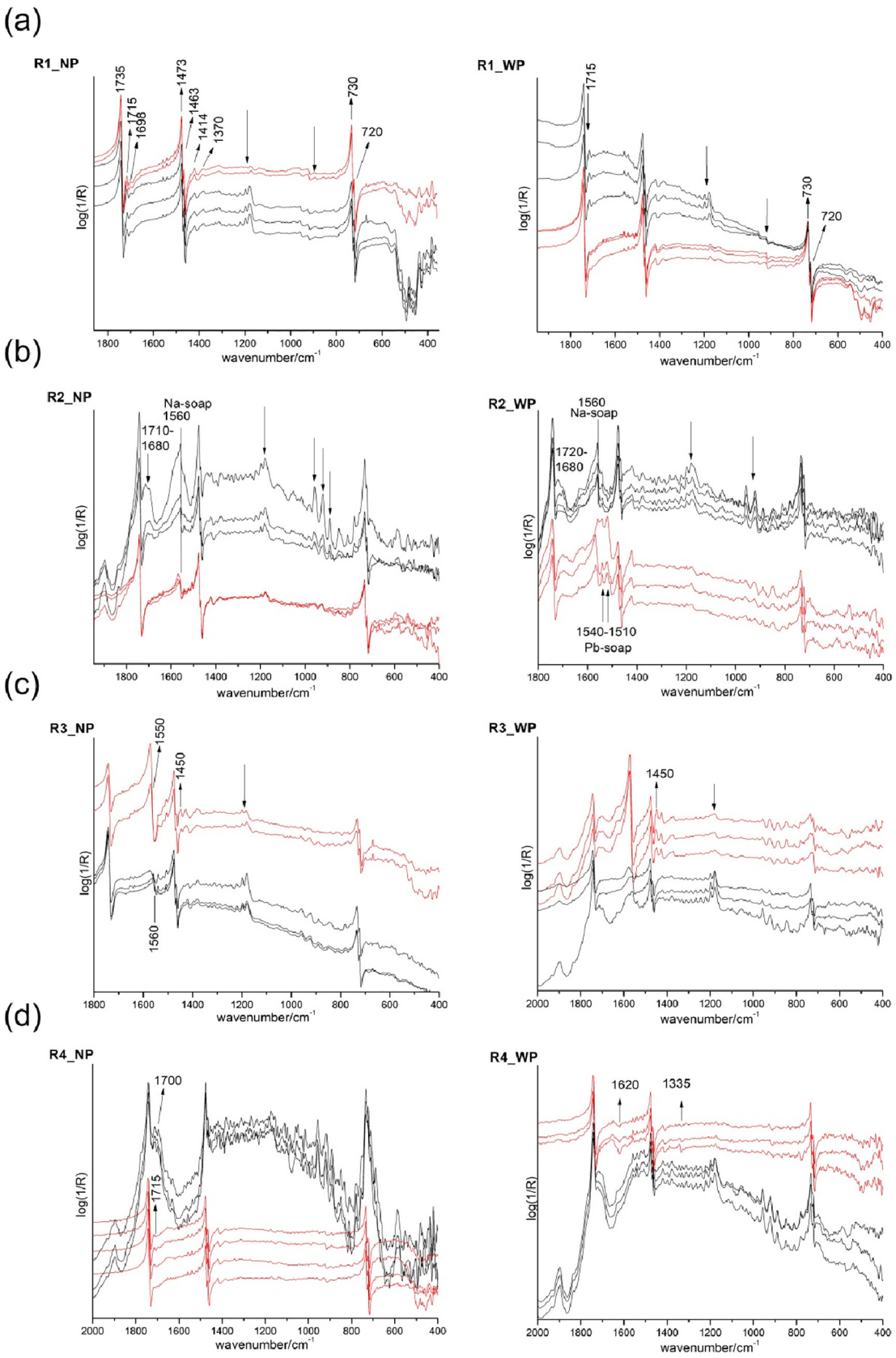

Fig. 12. FTIR spectra in reflection mode of: (a) Recipe 1 (R1) – pure beeswax, untreated; (b) Recipe 2 (R2) –Punic wax; (c) Recipe 3 (R3) – Alkali-treated wax; (d) Recipe 4 (R4) – Pure beeswax with added linseed oil soap; with no pigment (NP), and with pigment (WP), unaged (UA, black) and aged (A, red).

Nevertheless the scope for differentiating encaustic recipes is limited in ancient samples. It is clear that detection of soaps in general cannot be considered indicative of the use of a saponified wax medium although identification of metal cations would allow these to be linked to a pigment origin. Sodium soaps may originate from processing but are equally attributable to emulsified (R3) or clarified (R2) waxes so are not indicative of the preparation of the medium.

3.4.2. Non-invasive reflection mode

As discussed above, the FTIR analyses performed using macro ATR on microsamples taken from the model materials were vital in determining the differences between the recipes, particularly in terms of specifically identifying the nature of soap species present.

An important aim of this work was also to verify if the same level of information can be accessed by analysing the model materials non-invasively using FTIR in reflection mode. Thus the materials were additionally analysed using this technique in both the medium (Fig. 12) and near infrared ranges (not discussed in this work). The main differences observed, as compared to the data acquired as a result of sampling and in macro ATR, and the diagnostic capabilities of the method are evaluated.

Spectral changes due to ageing, possibly linked to a diminishing of the ordered structure of the aliphatic chains in beeswax, were observed in all the samples investigated, both pigmented and unpigmented. This increase of conformational disorder is reflected by the diminishing of the progression CH_2 wagging and rocking bands in the range 1400–1300 cm^{-1} and 1000–800 cm^{-1} (Fig. 12, indicated by arrows) [44,45]. These changes are not visible in the macro ATR spectra, perhaps indicating that they are limited to the surface of the sample, which is probed by this method.

The formation of sodium soaps, mainly evidenced by the band at c. 1560 cm^{-1}, is also observed by this technique in the spectra of the unaged, pigmented and unpigmented samples treated with sodium bicarbonate (R2 and R3; Fig. 12(b) and (c), left). In agreement with ATR-FTIR measurements, this band is observed to change with ageing, resulting in reflection mode, in an up-shifted and sharp derivative peak (Fig. 12(b) and (c), right) [46]. This could be related to a change in the composition of the sodium carboxylates present on ageing, also manifested in the macro ATR spectra.

Although evidence for the formation of lead soaps upon addition of the red lead pigment is also observed by this technique, this is less clear-cut for certain samples than in the equivalent spectra acquired using macro ATR. Thus, the bands at 1539 and 1511 cm^{-1}, assigned to the asymmetric stretches of the lead carboxylate species, and observed in the macro ATR spectra of the pigmented R1 samples (both unaged and aged - Fig. 6(a); R1_WP_UA and Fig. 9(a); R1_WP_A), do not appear to be visible in the reflection mode spectra (Fig. 12(a), right). A similar consideration can be made for the pigmented R4 samples, both aged and unaged (Fig. 12(d)).

For samples R2 and R3 non-invasive FTIR spectroscopy is in agreement with ATR-FTIR results (Fig. 12 (b) and (c)).In the case of the samples from R3, lead carboxylates bands are not observed with either the non-invasive FTIR and ATR-FTIR methods (Fig. 6(c); R3_WP_A). In the pigmented R2 sample, lead carboxylates, visible at 1540 and 1510 cm^{-1}, are detected by non-invasive FTIR even before the ageing and increase following ageing (Fig. 12(b) right).

The disagreement among the macro ATR and reflection modes in the case of R1 and R4 in the detection of lead carboxylates (visible only by macro ATR) could be explained by a preferential localization of the metal soap in the bulk of the material rather than on the surface.

This highlights the need to continue these fundamental studies into the characterisation of model materials using both invasive and non-invasive methodologies, in order to understand soap formation in encaustic media and underpin observations made non-invasively. It would be particularly pertinent to extend the study to model systems with pigments used widely in encaustic painting and containing cations other than lead, such as calcium, iron and copper.

Once these fundamental characterisation studies are in place, a major advantage of the non-invasive approach would be the ability to carry out a more representative survey of a surface painted in encaustic, unrestricted by the caveats of sampling, which would thus be able to access more of the palette. Although less molecular detail would be forthcoming from these studies than would be gleaned from the suite of destructive analyses detailed in this work, this would be set against the much larger amount of data that could be gathered from the entire surface of many more works, information which could be used to further the understanding of ancient encaustic painting techniques.

The study also underlined the ability of the FTIR reflection mode method to simultaneously provide information on the surface properties, both in terms of chemical composition and degree of structural order/disorder of the paint layer, and how these are affected by ageing and the presence of other cations.

4. Conclusions

This study has demonstrated differences in composition of encaustic media brought about by the wax processing technique and consequent impact on their working properties as paints and visual appearance after ageing. In some cases the working and ageing properties would preclude their viable utility as painting media and the use of these materials can thus be questioned on practical grounds. In terms of composition, differences between Recipes 2 and 3 were subtle compared with differences between these and Recipes 1 and 4; soap formation is the most significant alteration but this study shows that detection of soaps in general cannot be considered indicative of the use of a saponified wax medium, because the sodium soaps that originate from processing may be equally attributable to emulsified (R3) or clarified (R2) waxes. Thus the scope for differentiating encaustic recipes is limited in ancient samples. Nevertheless, identification of metal cations can allow soaps to be linked to a pigment origin and more research with a wider range of pigments is now desirable to further probe the exchange rates or equilibria operating within other pigment (metal) systems.

Strengths and weakness of the analytical approaches employed have been tested by this work and the necessity of adopting methods that detect and diagnose soap species has been shown to be crucial for understanding the composition and behaviour of encaustic media. The study has highlighted the benefit of an integrated multi-analytical approach and the importance of insights from invasive study to evaluating the results of non-invasive analysis of ancient encaustic painted surfaces.

Acknowledgements

This work was undertaken within the IPERION-CH project (Integrated Platform for the European Research Infrastructure ON Cultural Heritage) which is funded by the European Commission, H2020-INFRAIA-2014-2015, under Grant No. 654028.

References

[1] J. Cuní, P. Cuní, B. Eisen, R. Savizky, J. Bove, Characterization of the binding medium used in Roman encaustic paintings on wall and wood, Anal. Methods 4 (2012) 659–669.
[2] A. Andreotti, I. Bonaduce, M.P. Colombini, A.L. Tenorio, E. Ribechii, M. Zanaboni, A GC/MS method to determine acid salts in Punic wax, in: S. Omarini (Ed.), Encausto : Storia, Tecniche e Ricerche = Encaustic : History, Technique and Research, Nardini, Firenze 2012, pp. 78–81.
[3] H. Kühn, Detection and identification of waxes, including Punic wax, by infra-red spectrography, Stud. Conserv. 5 (1960) 71–81.
[4] G. Botticelli, A. Freccero, M. Matteini, Reproduction of pictorial techniques using beeswax, Punic wax, encasutic and other, in: S. Omarini (Ed.), Encausto : Storia, Tecniche e Ricerche = Encaustic : History, Technique and Research, Nardini, Firenze 2012, pp. 141–151.
[5] B. Ramer, The technology, examination and conservation of the Fayum portraits in the Petrie Museum, Stud. Conserv. 24 (1) (1979) 13.

[6] R.J. Stacey, The composition of some roman medicines: evidence for Pliny's Punic wax? Anal. Bioanal. Chem. 401 (2011) 1749.
[7] R. White, The application of gas-chromatography to the identification of waxes, Stud. Conserv. 23 (1978) 57–68.
[8] S. Colinart, S. Grappin-Wsevolojsky, La cire punique: étude critique des recettes antiques et de leur interprétation, Application aux portraits du Fayoum, Triennial meeting (12th), Lyon, 29 August-3 September 1999: Preprints, Vol. 1, James & James 1999, pp. 213–220.
[9] L. Robinet, M.-C. Corbeil, The characterization of metal soaps, Stud. Conserv. 48 (2003) 23–40.
[10] A. Freccero, Wax paint and punic wax - research and experiment, in: S. Omarini (Ed.), Encausto : Storia, Tecniche e Ricerche = Encaustic : History, Technique and Research, Nardini, Firenze 2012, pp. 105–113.
[11] I. Bonaduce, L. Carlyle, M.P. Colombini, C. Duce, C. Ferrari, E. Ribechini, P. Selleri, M.R. Tiné, New insights into the ageing of linseed oil paint binder: a qualitative and quantitative analytical study, PLoS One 7 (2012), e49333.
[12] S.A. Centeno, D. Mahon, The chemistry of aging in oil paintings: metal soaps and visual changes, The Metropolitan Museum of Art Bulletin 67 (2009) 12–19.
[13] G. Osmond, K. keune, J. Boon, A study of zinc soap aggregates in a late 19th century painting by R.G. Rivers at the Queensland art gallery, AICCM Bulletin 29 (2005) 37–46.
[14] C. Cartwright, A. Middleton, Scientific aspects of ancient faces: mummy portraits from Egypt, British Museum Technical Research Bulletin 2 (2008) 59–66.
[15] I. Bonaduce, M.P. Colombini, Characterisation of beeswax in works of art by gas chromatography–mass spectrometry and pyrolysis–gas chromatography–mass spectrometry procedures, J. Chromatogr. A 1028 (2004) 297–306.
[16] J. Mazurek, Free Fatty Acid Profiles in Water Sensitive Oil Paints: A Comparison of Modern and 15th-Century Oil Paints, American Institute of Conservation 42nd Annual Meeting San Francisco, CA. 2014 215–238.
[17] J. Mazurek, M. Svoboda, J. Maish, K. Kawahara, S. Fukakusa, T. Nakazawa, Y. Taniguchi, Characterization of binding media in Egyptian Romano portraits using enzyme-linked immunosorbant assay and mass spectrometry, e-preservation, Science 11 (2014) 76–83.
[18] M. Schilling, Paint Media Analysis, Scientific Examination of Art: Modern Techniques in Conservation and Analysis, National Academies Press, Washington DC, 2005 186–204.
[19] V.Y. Birshtein, V.M. Tul'chinskii, Determination of beeswax and some impurities by IR spectroscopy, Chem. Nat. Compd. 13 (1977) 232–235.
[20] H.L. Casal, H.H. Mantsch, D.G. Cameron, R.G. Snyder, Interchain vibrational coupling in phase II (hexagonal) n-alkanes, J. Chem. Phys. 77 (1982) 2825–2830.
[21] R.G. Snyder, Vibrational correlation splitting and chain packing for the crystalline n-alkanes, J. Chem. Phys. 71 (1979) 3229–3235.
[22] R.W. Corkery, A variation on Luzzati's soap phases. Room temperature thermotropic liquid crystals, Phys. Chem. Chem. Phys. 6 (2004) 1534–1546.
[23] C. Duce, S. Orsini, A. Spepi, M.P. Colombini, M.R. Tiné, E. Ribechini, Thermal degradation chemistry of archaeological pine pitch containing beeswax as an additive, J. Anal. Appl. Pyrolysis 111 (2015) 254–264.
[24] D. Balköse, T.O. Egbuchunam, F.E. Okieimen, Thermal behaviour of metal soaps from biodegradable rubber seed oil, J. Therm. Anal. Calorim. 101 (2010) 795–799.
[25] J.J. Hermans, K. Keune, A. van Loon, P.D. Iedema, An infrared spectroscopic study of the nature of zinc carboxylates in oil paintings, J. Anal. At. Spectrom. 30 (2015) 1600–1608.
[26] G. Hoffmann, CIELab color space, http://docs-hoffmann.de/cielab03022003.pdf, Accessed date: 18 December 2017.
[27] F.R.L. Schoening, The x-ray diffraction pattern and deformation texture of beeswax, S. Afr. J. Sci. 76 (1980) 262–265.
[28] J.J. Hermans, K. Keune, A. van Loon, R.W. Corkery, P.D. Iedema, Ionomer-like structure in mature oil paint binding media, RSC Adv. 6 (2016) 93363–93369.
[29] M. Cotte, E. Checroun, J. Susini, P. Dumas, P. Tchoreloff, M. Besnard, P. Walter, Kinetics of oil saponification by lead salts in ancient preparations of pharmaceutical lead plasters and painting lead mediums, Talanta 70 (2006) 1136–1142.
[30] A.A. Attama, B.C. Schicke, C.C. Müller-Goymann, Further characterization of theobroma oil–beeswax admixtures as lipid matrices for improved drug delivery systems, Eur. J. Pharm. Biopharm. 64 (2006) 294–306.
[31] Y. Gaillard, A. Mija, A. Burr, E. Darque-Ceretti, E. Felder, N. Sbirrazzuoli, Green material composites from renewable resources: polymorphic transitions and phase diagram of beeswax/rosin resin, Thermochim. Acta 521 (2011) 90–97.
[32] S. Aze, J.-M. Vallet, V. Detalle, O. Grauby, A. Baronnet, Chromatic alterations of red lead pigments in artworks: a review, Phase Transit. 81 (2008) 145–154.
[33] S. Aze, J.-M. Vallet, A. Baronnet, O. Grauby, The fading of red lead pigment in wall paintings: tracking the physico-chemical transformations by means of complementary micro-analysis techniques, Eur. J. Mineral. 18 (2006) 835–843.
[34] M. Cotte, E. Checroun, W.D. Nolf, Y. Taniguchi, L.D. Viguerie, M. Burghammer, P. Walter, C. Rivard, K. Janssens Murielle Salomé, J. Susini, Lead soaps in paintings: friends or foes? Stud. Conserv. 62 (2017) 2–23.
[35] N.J. Flemming, V.J. Lopata, B.L. Sanipelli, P. Taylor, Thermal decomposition of basic lead carbonates: a comparison of hydrocerussite and plumbonacrite, Thermochim. Acta 81 (1984) 1–8.
[36] F. Vanmeert, G. Van der Snickt, K. Janssens, Plumbonacrite identified by X-ray powder diffraction tomography as a missing link during degradation of red lead in a van Gogh painting, Angew. Chem. Int. Ed. 54 (2015) 3607–3610.
[37] M.H. Brooker, S. Sunder, P. Taylor, V.J. Lopata, Infrared and Raman spectra and X-ray diffraction studies of solid lead(II) carbonates, Can. J. Chem. 61 (1983) 494–502.
[38] D. Saunders, M. Spring, C. Higgitt, Colour change in red lead-containing paint films, ICOM Committee for Conservation, ICOM-CC : 13th Triennial Meeting, Rio de Janeiro, 22–27 September 2002: Preprints 2002, pp. 455–463.
[39] H. Howard, Pigments of English Medieval Wall Painting, Archetype, London, 2003.
[40] M. Cotte, P. Dumas, G. Richard, R. Breniaux, P. Walter, New insight on ancient cosmetic preparation by synchrotron-based infrared microscopy, Anal. Chim. Acta 553 (2005) 105–110.
[41] J.S. Mills, R. White, The Organic Chemistry of Museum Objects, Butterworth-Heinemann, Oxford; London; Boston, 1994.
[42] M. Regert, S. Colinart, L. Degrand, O. Decavallas, Chemical alteration and use of beeswax through time: accelerated ageing tests and analysis of archaeological samples from various environmental contexts, Archaeometry 43 (2001) 549–569.
[43] C. Heron, N. Nemcek, K.M. Bonfield, D. Dixon, B.S. Ottaway, The chemistry of neolithic beeswax, Naturwissenschaften 81 (1994) 266–269.
[44] A.N. Parikh, S.D. Gillmor, J.D. Beers, K.M. Beardmore, R.W. Cutts, B.I. Swanson, Characterization of chain molecular assemblies in long-chain, layered silver thiolates: a joint infrared spectroscopy and X-ray diffraction study, J. Phys. Chem. B 103 (1999) 2850–2861.
[45] R.N.A.H. Lewis, R.N. McElhaney, Membrane lipid phase transitions and phase organization studied by Fourier transform infrared spectroscopy, Biochim. Biophys. Acta Biomembr. 1828 (2013) 2347–2358.
[46] F. Rosi, A. Daveri, P. Moretti, B.G. Brunetti, C. Miliani, Interpretation of mid and near-infrared reflection properties of synthetic polymer paints for the non-invasive assessment of binding media in twentieth-century pictorial artworks, Microchem. J. 124 (2016) 898–908.